

# X-Ray Photon Correlation Spectroscopy Study of Brownian Motion of Gold Colloids in Glycerol

S. B. Dierker,<sup>1</sup> R. Pindak,<sup>2</sup> R. M. Fleming,<sup>2</sup> I. K. Robinson,<sup>3</sup> and L. Berman<sup>4</sup>

<sup>1</sup>*Department of Physics, University of Michigan, Ann Arbor, Michigan 48109-1120*

<sup>2</sup>*AT&T Bell Laboratories, 600 Mountain Avenue, Murray Hill, New Jersey 07974-0636*

<sup>3</sup>*Department of Physics, University of Illinois at Urbana-Champaign, Urbana, Illinois 61801-3080*

<sup>4</sup>*National Synchrotron Light Source, Brookhaven National Laboratory, Upton, New York 11973-5000*

(Received 30 November 1994; revised manuscript received 5 May 1995)

We report x-ray photon correlation spectroscopy studies of the static structure factor and dynamic correlation function of a gold colloid dispersed in the viscous liquid glycerol. We find a diffusion coefficient for Brownian motion of the gold colloid which agrees well with that extrapolated from measurements made with visible light, but which was determined on an optically opaque sample and in a wave-vector range inaccessible to visible light.

PACS numbers: 61.10.Lx, 05.40.+j, 42.25.Kb, 82.70.Dd

Photon correlation spectroscopy (PCS) probes the dynamics of a material by analyzing the temporal correlations among photons scattered by the material. Visible light PCS has proven to be an indispensable technique for studying the long wavelength hydrodynamics of fluids, including simple liquids, liquid mixtures, liquid crystals, polymers, and colloids [1]. However, visible PCS cannot probe the short wavelength dynamics of materials or opaque materials at all. The new field of x-ray PCS (XPCS) offers an unprecedented opportunity to extend the range of length scales over which a material's low frequency ( $10^{-3}$  to  $10^6$  Hz) dynamics can be probed down to interatomic spacings. It is clear that demonstration of the ability to make dynamic XPCS measurements would be a major step forward in this nascent field.

Many of the important problems in the low frequency dynamics of condensed matter systems for which XPCS should be uniquely suited arise in disordered materials, in particular, liquids. These include studies of the dynamic structure factor of liquids down to interatomic length scales, density fluctuations in liquids undergoing a glass transition, internal conformational dynamics and reptation in polymers, and equilibrium concentration fluctuations in polymer blends near a phase separation critical point. Here we report results of equilibrium dynamic measurements on a disordered system using XPCS. Specifically, we measured the diffusion coefficient for Brownian motion of gold colloid particles dispersed in glycerol. Our results unequivocally demonstrate the feasibility of the XPCS technique, as well as illustrate the crucial importance of both matching the longitudinal coherence length of the x rays to the experimental requirements and the tremendous benefit of utilizing area detectors in XPCS measurements.

While the principles of XPCS have been known for decades, the very low flux of coherent x rays available with previous sources has, until now, precluded its application as a practical technique. The critical development which has now made XPCS a feasible technique is the use of insertion devices at second and third generation

synchrotron sources. The work reported here was done on the wiggler beam line X25 at the Brookhaven National Synchrotron Light Source (NSLS).

Previous work has consisted of measurements of the static speckle patterns resulting from the structure of antiphase domains in  $\text{Cu}_3\text{Au}$  [2] or from grazing incidence scattering from gold-coated polymer films of inhomogeneous thickness [3]. Identification of equilibrium critical fluctuations in  $\text{Fe}_3\text{Al}$  with XPCS has also been reported very recently [4]. These studies benefited either from the tremendous gain in scattering cross section of Bragg scattering from essentially well-ordered materials [2,4] or from the large reflectivity at grazing incidence [3]. In contrast, the scattering typical of highly disordered materials, such as liquids or glasses, is dramatically weaker.

To demonstrate the difficulty of a coherent x-ray beam by liquids, we estimate its average scattering efficiency. For an incident x-ray beam of cross-sectional area  $A_i$  and power  $P_0$  (photons/sec) incident on a sample containing  $N_{\text{tot}}$  uncorrelated atoms of charge  $Z$ , the fractional detected count rate ( $P/P_0$ ) scattered into the solid angle  $\Delta\Omega$  is [5]  $P/P_0 = r_0^2 N_{\text{tot}} Z^2 \Delta\Omega / A_i$ . Here  $r_0 = e^2/mc^2 = 2.8 \times 10^{-13}$  cm is the classical Thomson electron radius. In terms of the density  $\rho$ , molecular weight  $M$ , Avogadro's number  $N_A$ , and the scattering volume  $V$ , we have  $N_{\text{tot}} = \rho V N_A / M$ . We take  $V = A_i / \mu$  for a sample of thickness  $t = 1/\mu$ , where  $\mu = \rho \mu_m$  is the adsorption length and  $\mu_m$  is the mass absorption coefficient, and make use of the approximate relationship [5]  $\mu_m \approx CZ\lambda^3 N_A / M$ , where  $C$  is a constant. In a speckle experiment, the detector solid angle of a single speckle is  $\Delta\Omega \approx \lambda^2 / A_i$ . Altogether this gives  $P/P_0 \approx 8 \times 10^{-26} Z / C \lambda A_i$ . This demonstrates the benefit of having a high source brightness, i.e.,  $P_0/A_i$ .  $A_i$  is set by the transverse coherence length of the x-ray beam. At X25, this requires a pinhole diameter of  $5 \mu\text{m}$ , for which  $A_i \sim 20 \mu\text{m}^2$ . For the case of liquid Au,  $Z = 79$ , and taking  $\lambda = 1.55 \text{ \AA}$  at 8 keV,  $C = 261 \text{ cm}^{-1}$  for Au at 8 keV, and  $P_0 \approx 4 \times 10^7$  photons/sec at X25 with  $\Delta E/E = 1.5\%$ , we estimate the impracticably small count rate of  $P \sim 3 \times 10^{-4}$  cps.

However, if one had a liquid of  $N_p$  gold particles, each with  $n_a$  atoms (whether crystalline or amorphous, regardless of orientation), such that  $N_p n_a = N_{\text{tot}}$ , then the average scattering in the forward direction would be the sum of the coherent scattering from  $N_p$  particles, i.e.,  $P/P_0 \propto N_p n_a^2 = N_{\text{tot}} n_a$ , instead of  $N_{\text{tot}}$ . The  $q$  dependence of the scattering will be that of the particle form factor [5]  $F(qR)$  for a sphere of radius  $R$  (in the dilute gas limit at low  $q$ , the structure factor will be unity),

$$F(qR) = \left[ \frac{3\{\sin(qR) - qR \cos(qR)\}}{(qR)^3} \right]^2. \quad (1)$$

For example, for a Au particle with  $R = 200 \text{ \AA}$ ,  $n_a \sim 2 \times 10^6$ , giving a sufficiently large  $P \sim 600$  photons/sec. A constraint of this approach is that one must work at very low  $q$ , although not so low as to be dominated by the tail of the Fraunhofer diffraction of the main beam. We estimate that measurements should be possible at least over the range  $1 \times 10^{-3} < q < 3 \times 10^{-2} \text{ \AA}^{-1}$ . This extends far beyond the upper  $q$  range of visible light scattering, for which  $q_{\text{max}} \sim 4 \times 10^{-3} \text{ \AA}^{-1}$ .

Monodisperse gold sols were prepared by reducing  $\text{HAuCl}_4$  with  $\text{Na}_3\text{-citrate}$  [6]. The hydrodynamic radius  $R_H$  of the resultant gold colloid particles was determined to be  $335 \text{ \AA}$  for a small diluted aliquot of the resulting sol using visible PCS [1]. A cumulant analysis of the dynamic correlation functions indicated a polydispersity of  $\sim 10\%$ . The hydrophobic gold sol was stabilized against aggregation by absorbing cold water fish skin gelatin onto the surface of the particles [7].  $R_H$  and the hydrodynamic polydispersity were remeasured for the stabilized sol and determined to be  $425 \text{ \AA}$  and  $20\%$ , respectively. The increased magnitude of these quantities presumably reflects the increased drag and statistical size fluctuations of the "fuzzy" molecular coat covering the spheres.

The as-prepared sol had a gold volume fraction of  $2.7 \times 10^{-4}\%$ , whereas the XPCS measurements required a sample with a gold volume fraction of  $\sim 1\%$ . At this concentration, the x-ray absorption of the gold and the glycerol are approximately equal. Thus,  $450 \text{ ml}$  of sol was concentrated by centrifuging, aspirating out the supernatant, and resuspending in  $1.5 \text{ ml H}_2\text{O}$  by ultrasonication. The concentrated sol was remeasured with visible PCS, and  $R_H$  and the polydispersity were determined to be  $590 \text{ \AA}$  and  $26\%$ , respectively. The sol was then centrifuged and the supernatant was aspirated and resuspended by ultrasonication in  $0.10 \text{ ml}$  glycerol to which  $0.4M$  NaCl had been added in order to screen out Coulomb interactions between the spheres. This was repeated twice more. The end result was a concentration enhancement of  $4000:1$ , giving an estimated gold volume fraction of  $1.3\%$  in a  $0.1 \text{ ml}$  sol. This concentration was confirmed by x-ray absorption measurements. We note that at this high concentration the sample is completely opaque to visible light, and thus could not be studied with visible PCS. The  $1\%$  Au sample was placed in a  $1.0 \text{ mm}$  diameter hole drilled in a  $0.6 \text{ mm}$  thick aluminum plate, i.e., about one absorption length thick at  $8 \text{ keV}$ .

A laterally coherent beam was prepared by passing the x rays through a  $5 \text{ \mu m}$  diameter pinhole. The longitudinal coherence length  $l_{\text{coh}}$  of the x-ray beam is given by  $\lambda(\lambda/\Delta\lambda)$  and was set by using a two crystal W/B<sub>4</sub>C multilayer monochromator, giving  $l_{\text{coh}} \sim 100 \text{ \AA}$ . This resulted in an incident coherent x-ray flux of  $4 \times 10^7$  photons/sec. In a transmission geometry, the maximum path length difference (PLD) is given by  $2h \sin\theta \tan\theta$ , where  $h$  is the sample thickness. Thus, the requirement [1] that  $\text{PLD} < l_{\text{coh}}$  is satisfied up to scattering angles  $2\theta$  of  $8 \text{ mrad}$ , corresponding to  $q = 3.2 \times 10^{-2} \text{ \AA}^{-1}$ . We also attempted measurements using a Si(220) monochromator, for which  $l_{\text{coh}} = 2 \text{ \mu m}$  and the incident coherent flux was only  $\sim 2 \times 10^5$  photons/sec. Data collected under those conditions were of significantly poorer quality than those reported here. However, small-angle scattering data collected under incoherent illumination conditions using the Si(220) monochromator were of good quality, and all such data presented here (Figs. 1–3) were collected using this monochromator. This underscores the crucial importance of not having  $l_{\text{coh}}$  any greater than required by PLD in order to have the maximum intensity available for the experiment.

X-ray detectors used included a scintillation detector and a two-dimensional charged couple device (CCD) area detector operated in the direct detection mode. The CCD detector was custom-built and used a Kodak KAF-1400 CCD, which is a front illuminated device having a  $512 \times 768$  array of  $9 \text{ \mu m}$  square pixels.

Figure 1 shows the measured scattering intensity, both with and without the colloid. The strong signal centered at  $q = 0$  is the direct beam transmitted through the sample. The background scattering without sample is due to small angle scattering from the slits and pinholes in the beam line. The overall shape and intensity of the colloid scattering qualitatively matches that expected from Eq. (1).

Measurements of the static structure factor were also made with the CCD area detector. Figure 2 shows a plot of a CCD image taken with an  $80 \text{ \mu m}$  front pinhole. The channel cut through the center of the plot is due to the shadow of a  $200 \text{ \mu m}$  diameter gold wire used to block the main beam, which would have saturated the

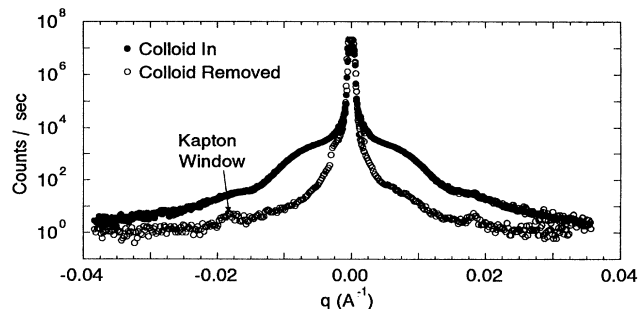


FIG. 1.  $S(q)$  as measured with incoherent x rays by scanning an  $80 \text{ \mu m}$  pinhole followed by a scintillation detector. The incident beam diameter was  $200 \text{ \mu m}$ . One contribution to the background, a Kapton window, is indicated.

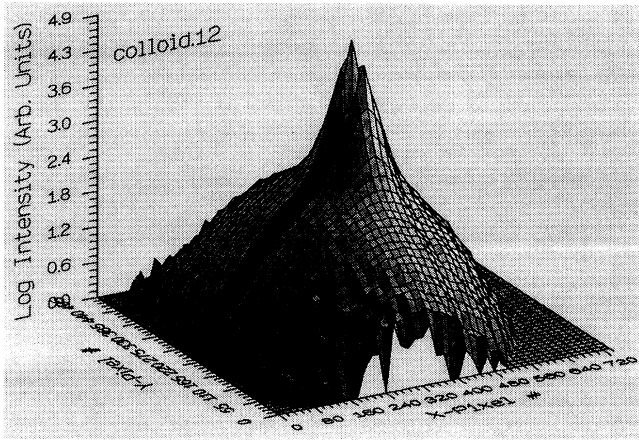


FIG. 2. Log plot of scattering intensity from the colloid collected with the CCD camera.

detector. The CCD image was obtained by summing ten 1 sec exposures in order to extend the CCD's dynamic range. In comparison, each line scan with the pinhole-scintillation detector combination over a similar  $q$  range took more than an hour.

A comparison of the structure factor measured in the scintillation detector scans with that deduced from radial averages of the CCD image is shown in Fig. 3. The data have been scaled to coincide at  $q \sim 0.015 \text{ Å}^{-1}$ . The scintillation detector and CCD scans show good general agreement apart from differences in the amount of forward scatter around the main beam between the two measurements.

In order to determine the size of the protected colloid spheres and the degree of polydispersity, the scintillation detector data shown in Fig. 3 were fit by a model consisting of a Gaussian distribution of sphere scattering radii, with each sphere according to Eq. (1), along with

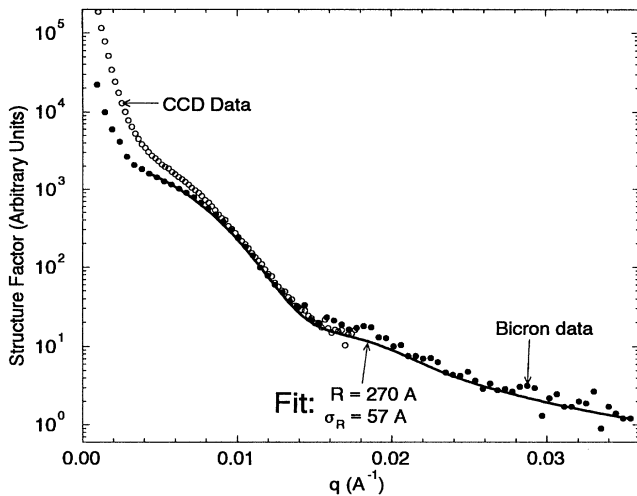


FIG. 3. Comparison of  $S(q)$  derived from scintillator or pinhole scans with that from the CCD image in Fig. 2. Also shown are the results of a fit of a model for  $S(q)$  based on Eq. (1) and a Gaussian distribution of particle radii.

a constant background. The results indicate that the mean radius was  $270 \text{ Å}$  and the standard deviation of the distribution was  $57 \text{ Å}$ . These numbers agree well with the mean hydrodynamic radius and polydispersity measured on dilute aqueous solutions of the colloid with visible PCS before protecting them with gelatin. This suggests that the increased  $R_H$  measured for the protected colloid results from the added hydrodynamic drag of the macromolecular coating. The further increase in  $R_H$  upon centrifuging presumably results from changes in the molecular conformation of the gelatin molecules and not from aggregation of the spheres.

We next turn to consideration of the Brownian motion dynamics of this system. The Au colloid particles form a dilute gas having diffusively relaxing concentration fluctuation with a corresponding diffusion coefficient given by [1]  $D = k_b T / 6\pi\eta R_H$  and a relaxation time at wave vector  $q$  of  $\tau = 1/Dq^2$ . Glycerol is a prototypical glass former with a glass transition at  $T_g = -86^\circ \text{C}$ , at which the shear viscosity  $\eta$  approaches  $\sim 10^{13} \text{ P}$  [8].

The dynamic correlation function  $g(t)$  is defined as

$$g(t) = \langle n(t)n(0) \rangle / \langle n(0) \rangle^2, \quad (2)$$

where  $\langle \rangle$  represents a time average and  $n(t)$  is the detected photon count at time  $t$ .  $g(t)$  should have a maximum value of 2 at  $t = 0$ , decaying to 1 at infinite time. Spatial averaging of the speckles by the detector can reduce the  $t = 0$  intercept of  $g(t)$ .

A dramatic increase in collection efficiency was obtained by using the CCD detector to measure the scattering for 6750 pixels simultaneously. Since the dynamics depend only on the magnitude of  $q$ , we can average the autocorrelation functions measured in all of the pixels in a band of  $q$  values. This is equivalent to performing an ensemble average over pixels, as well as a time average for each pixel, and should reduce the time needed to measure the correlation functions with good statistics by the number of pixels averaged over [9]. With 6750 pixels/image, the reduction is substantial.

Specifically, we recorded 1920 images of the intensity in two separate  $90^\circ$  arcs corresponding to  $q$ 's of  $3.3 \times 10^{-3}$  and  $5.5 \times 10^{-3} \text{ Å}^{-1}$ , with widths of 10% of their average  $q$ 's and containing 1750 and 5000 pixels, respectively (see Fig. 4). The larger  $q$  is well above the maximum value of  $\sim 4 \times 10^{-3} \text{ Å}^{-1}$  attainable by visible PCS. The images were taken once per second for a total duration of 32 min, with the exact time of exposure recorded for each image. A total of  $\sim 3.4 \times 10^6$  photons were detected, corresponding to an average count rate of 0.36 photons/pixel sec. This compares well with the value of 0.68 derived from our earlier estimate when the sample transmission (0.35), the ratio of the area of a pixel to that of a speckle (0.13), the estimated quantum efficiency of the CCD detector (0.05), and Eq. (1) (0.5) are taken into account.

The time autocorrelation function of each pixel was then calculated and the ensemble average of the resulting 1750

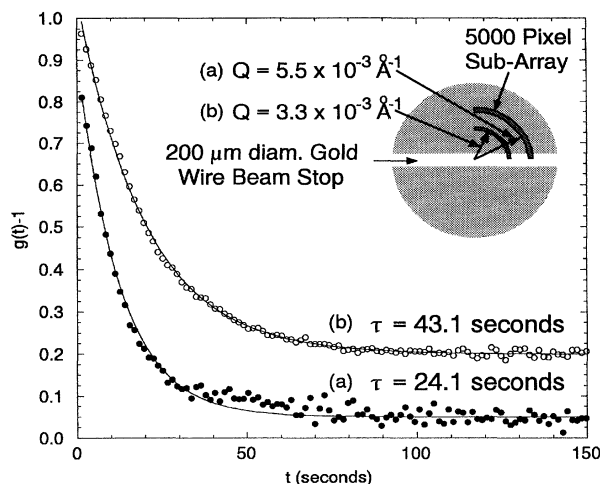


FIG. 4. Autocorrelation functions of colloid scattering intensity as collected with the CCD camera for two different wave vectors along with single exponential fits and relaxation times, as indicated. The inset schematically depicts the scattering "halo," the beam stop, and the subarrays which were ensemble averaged over. Curve (b) is offset by 0.15 for clarity.

or 5000 correlation functions calculated. The results are shown in Fig. 4, which is plotted as  $g(t) - 1$ . The large signal-to-noise ratio of the data in Fig. 4 can leave no doubt that they correspond to dynamic x-ray scattering from colloid concentration fluctuations. The large amplitude of the decays is also as expected considering the small size of the pixels relative to the coherence area for the scattering.

Also shown in Fig. 4 are fits to the data of single exponential relaxations. They give characteristic decay times of 43.1 and 24.1 sec for  $q = 3.3 \times 10^{-3}$  and  $5.5 \times 10^{-3} \text{ \AA}^{-1}$ , respectively. The measurements were made at a temperature of  $-29^\circ\text{C}$ . The viscosity of pure glycerol [8] should be  $5.5 \times 10^3 \text{ P}$  at this temperature. Thus, the nominal expected relaxation times are 61 and 22 sec, which are in good agreement with the measurements. The deviation of the relaxation rates from a precise  $q^2$  dependence may be an indication of the onset of nonhydrodynamic effects at large wave vector [10].

While these measurements clearly establish the feasibility of XPCS studies, more experiments are called for in order to fully understand the dynamics of this colloid. For example, nonhydrodynamic effects at large wave vector [10] as well as nonlinear relaxation effects predicted by mode coupling theories [11] near the glass transition should be fruitful areas of future study with this new technique.

In conclusion, we have made small angle x-ray scattering measurements of the static structure factor of an optically opaque gold colloid dispersed in glycerol. We also reported a determination of dynamic correlation functions and the diffusion coefficient for the Brownian motion of the colloid particles, at a wavelength inaccessible to visible PCS, by using the new technique of XPCS. Our

results demonstrate the importance of using a multilayer monochromator, or just the natural bandwidth of undulator radiation ( $\sim 1\%$ ), in situations where a large  $l_{\text{coh}}$  is not required, such as surface diffraction or small-angle scattering experiments, as well as the benefits of ensemble averaging with CCD area detectors in XPCS measurements.

The present results clearly show that XPCS is a feasible technique and can have wide application to certain classes of systems, especially complex fluids and surfaces, even using existing 2nd generation synchrotron x-ray sources such as the NSLS. This is particularly true given several significant forthcoming enhancements: (1) Optimization of the use of an area detector for making ensemble measurements of  $g(\tau)$ :  $\times 10^1 - 10^2$ . (2) Beam-line optics which utilize the full coherent output of the undulator in both the vertical and horizontal directions:  $\times 10$ . (3) Introduction of undulator sources such as the Prototype Small Gap Undulator recently installed at the NSLS:  $\times 10$ . These will enhance the data collection efficiency by  $10^3$  and  $10^4$ , relative to the current experiment. Those classes of problems demanding the utmost coherent incident x-ray flux will require the 3rd generation undulator sources at the European Synchrotron Radiation Facility and the Advanced Photon Source:  $\times 10^2 - 10^3$ , for a total gain of  $10^4 - 10^6$ , relative to the current experiment. When these developments come to fruition, XPCS will realize its full potential as a unique and important new technique.

It is a pleasure to acknowledge the assistance and advice of Christoph Schmidt on the preparation of the gold colloids. Robert MacHarrie assisted in the x-ray measurements. S.B.D. acknowledges support under NSF Grant No. DMR 92-17956 and also the donors of the Petroleum Research Fund, administered by the American Chemical Society, for the partial support of this research under Grant ACS-PRF No. 26389-AC9. I.K.R. acknowledges support under NSF Grant No. DMR 93-15691. The NSLS is supported by the U.S. Department of Energy under Contract No. DE-AC02-76CH00016.

- [1] See, for example, Benjamin Chu, *Laser Light Scattering: Basic Principles and Practices* (Academic Press, San Diego, 1991), 2nd ed.
- [2] M. Sutton *et al.*, *Nature* (London) **352**, 608 (1991).
- [3] Z. H. Cai *et al.*, *Phys. Rev. Lett.* **73**, 82 (1994).
- [4] S. Brauer *et al.*, *Phys. Rev. Lett.* **74**, 2010 (1995).
- [5] G.B.E. Warren, *X-Ray Diffraction* (Addison-Wesley, New York, 1968).
- [6] G. Frens, *Nature* (London) **241**, 20 (1973).
- [7] *Colloidal Gold: Principles, Methods, and Applications*, edited by M.A. Hayat (Academic Press, San Diego, 1989).
- [8] M.L. Williams *et al.*, *J. Phys. Chem.* **77**, 3701 (1955).
- [9] Apollo P. Y. Wong and P. Wiltzius, *Rev. Sci. Instrum.* **64**, 2547 (1993).
- [10] W. Hess and R. Klein, *Adv. Phys.* **32**, 214 (1983).
- [11] J. Jackle, *J. Phys. Condens. Matter* **1**, 267 (1989).

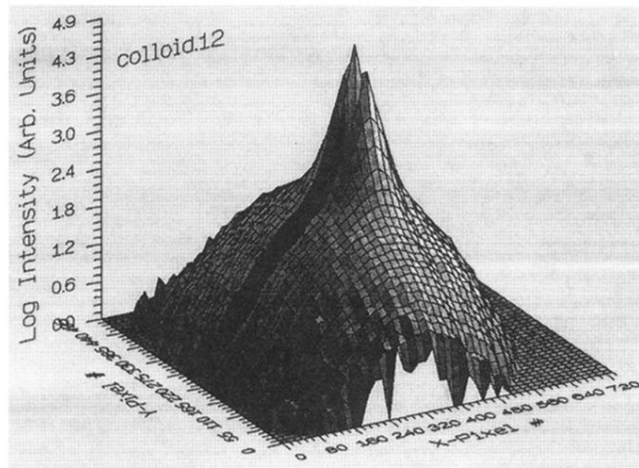


FIG. 2. Log plot of scattering intensity from the colloid collected with the CCD camera.